Impaired contractile responses and altered expression and phosphorylation of Ca^{2+} sensitization proteins in gastric antrum smooth muscles from *ob/ob* mice

Bhupal P. Bhetwal, **Changlong An**, **Salah A. Baker**, **Kristin L. Lyon**, and **Brian A. Perrino**
Department of Physiology & Cell Biology, Center of Biomedical Research Excellence, University of Nevada School of Medicine, CMM 203E—MS 0575, 1664 N Virginia St, Reno, NV 89557, USA

Abstract

Diabetic gastroparesis is a common complication of diabetes, adversely affecting quality of life with symptoms of abdominal discomfort, nausea, and vomiting. The pathogenesis of this complex disorder is not well understood, involving abnormalities in the extrinsic and enteric nervous systems, interstitial cells of Cajal (ICCs), smooth muscles and immune cells. The *ob/ob* mouse model of obesity and diabetes develops delayed gastric emptying, providing an animal model for investigating how gastric smooth muscle dysfunction contributes to the pathophysiology of diabetic gastroparesis. Although ROCK2, MYPT1, and CPI-17 activities are reduced in intestinal motility disorders, their functioning has not been investigated in diabetic gastroparesis. We hypothesized that reduced expression and phosphorylation of the myosin light chain phosphatase (MLCP) inhibitory proteins MYPT1 and CPI-17 in *ob/ob* gastric antrum smooth muscles could contribute to the impaired antrum smooth muscle function of diabetic gastroparesis. Spontaneous and carbachol- and high K^+-evoked contractions of gastric antrum smooth muscles from 7 to 12 week old male *ob/ob* mice were reduced compared to age- and strain-matched controls. There were no differences in spontaneous and agonist-evoked intracellular Ca^{2+} transients and myosin light chain kinase expression. The F-actin:G-actin ratios were similar. Rho kinase 2 (ROCK2) expression was decreased at both ages. Basal and agonist-evoked MYPT1 and myosin light chain 20 phosphorylation, but not CPI-17 phosphorylation, was reduced compared to age-matched controls. These findings suggest that reduced MLCP inhibition due to decreased ROCK2 phosphorylation of MYPT1 in gastric antrum smooth muscles contributes to the antral dysmotility of diabetic gastroparesis.

Keywords

Diabetic gastroparesis; ROCK2; CPI-17; MYPT1; Ca^{2+} sensitization

Introduction

Gastroparesis is characterized by abnormal gastric function resulting in delayed gastric emptying in the absence of mechanical or physical obstruction (Parkman et al. 2004). Diabetic gastroparesis is increasingly being diagnosed in patients with type 2 diabetes, which constitute 90–95 % of the diabetic population, and now represents nearly 30 % of all

cases of gastroparesis (Soykan et al. 1998; Wang et al. 2008). Diabetic gastroparesis can cause debilitating symptoms of nausea, and vomiting, and is associated with significant morbidities, including nutritional insufficiency, electrolyte imbalance, and impaired glycemic control (Intagliata and Koch 2007). Diabetic gastroparesis has an adverse effect on the patients' quality of life, and represents a major health care burden due to costly care and frequent hospitalizations (Intagliata and Koch 2007).

The pathogenesis of diabetic gastroparesis is not well understood, involving abnormalities in the extrinsic and enteric nervous systems, interstitial cells of Cajal (ICCs), smooth muscles and immune cells (Hasler 2011). In patients with diabetic gastroparesis, fasting and fed antral contractions are reduced, and antral diameter is increased (Hasler 2011). Gastric smooth muscle dysfunction can occur as a result of hyperglycemia, insulopenia, and IGF-1 deficiency or unresponsiveness, leading to disruptions in smooth muscle protein expression and an altered smooth muscle phenotype (Horvath et al. 2006; Kashyap and Farrugia 2010). Antral smooth muscle degeneration and fibrosis, with increased connective tissue stroma and thickened basal lamina, along with abnormalities in smoothelin-A expression are common findings in gastric biopsy specimens from patients with diabetic gastroparesis (Ejskjaer et al. 1999; Grover et al. 2011). These studies indicate that impaired signal transduction in gastric smooth muscles may adversely affect antral motility in diabetic gastroparesis.

Ca^{2+} influx triggers gastrointestinal (GI) smooth muscle contraction and myosin regulatory light chain (LC20) phosphorylation, which reflects the net activity of myosin light chain kinase (MLCK) or myosin light chain phosphatase (MLCP) (Khromov et al. 2009; Sanders 2008). Regulating MLCP during Ca^{2+} influx contributes to the force generation of GI smooth muscles (Murthy 2006; Murthy et al. 2003; Somlyo and Somlyo 2003). MLCP inhibition by MYPT1 and/or CPI-17 phosphorylation favors LC20 phosphorylation and greater force generation at a given $[Ca^{2+}]_i$, and is referred to as $Ca^{2?}$ sensitization (Somlyo and Somlyo 2003). MYPT1 phosphorylation by Rho associated kinase 2 (ROCK2) at T696 and T853, and CPI-17 phosphorylation at T38 by protein kinase C (PKC) is the primary mechanism underlying the regulation of the Ca^{2+} sensitivity of the MLCK-driven force of smooth muscle contractions (Hirano 2007). Different GI tract organs utilize different mechanisms to generate tension or contractile activity in accordance with their function (Rattan et al. 2010). Dihydropyridines reduce spontaneous or basal circular smooth muscle contractions of several GI smooth muscles (Cobine et al. 2007; Kovac et al. 2005; Rich et al. 1993; Wegener et al. 2006). GI tract sphincters which generate tone are more sensitive to Rho kinase inhibition and have higher ROCK2 and CPI-17 levels, but lower MYPT1 levels than predominantly phasic smooth muscles (Patel and Rattan 2006). Further complexity arises from the expression of MYPT1 leucine-zipper positive or negative (LZ+/LZ–) isoforms involved in cGMP-dependent protein kinase-dependent relaxation, or RhoA targeting (Fu et al. 2012; Riddick et al. 2008).

These findings indicate that ROCK2, MYPT1, and CPI-17 expression levels are relevant factors in determining the importance of Ca^{2+} sensitization pathways to gastric smooth muscle contractile responses (Rattan et al. 2010; Sanders 2008). Impaired Ca^{2+} sensitization protein expression and activation have been reported in intestinal motility disorders (Depoortere et al. 2010; Godoy and Rattan 2011; Ohama et al. 2003; Sato et al. 2007). Similar to diabetes patients, delayed gastric emptying has been observed in animal models of diabetes including streptozotocin-induced diabetes in rats, and in genetically-induced diabetes of NOD, *db/db*, and *ob/ob* mice (Asakawa et al. 2003; Ordog et al. 2000; Xue and Suzuki 1997; Yamamoto et al. 2008). However, alterations in Ca^{2+} sensitization pathways affecting diabetic gastroparesis have not been reported. In this study we examined the expression levels of γ-actin, LC20, ROCK2, LZ-/LZ + MYPT1, CPI-17, and basal MYPT1,

CPI-17, and LC20 phosphorylation levels in gastric antrum smooth muscles from C57BL/6 J mice and *ob/ob* mice, a genetic model of obesity and type 2 diabetes (Ingalls et al. 1950). We found differences in the contractile responses and in the expression and phosphorylation of these MLCP regulatory proteins in gastric antrum smooth muscles from 7 to 12 week old wild-type mice and *ob/ob* mice. Investigations of GI smooth muscle regulation are necessary to expand the number of strategies available for treatment of GI motility disorders. These findings may facilitate studies aimed at further understanding the role of Ca^{2+} sensitization pathways in the pathophysiology of diabetic gastroparesis.

Materials and methods

Mice

Male C57BL/6J and *ob/ob* mice were purchased from The Jackson Laboratory (Bar Harbor, ME). The mice were maintained and experiments carried out in accordance with the National Institutes of Health Guide for the Care and Use of Laboratory Animals. Animal protocols were approved by the University of Nevada, Reno Institutional Animal Care and Use Committee. Mice were housed in a pathogen-free barrier facility on a 12-h light/dark cycle with free access to water and food (Prolab 5P76 Isopro 3000; 5.4 % fat by weight). Mice at 7 and 12 weeks of age were used for all experiments. Blood glucose measurements were performed with an Accu-Chek Complete monitor (Boehringer Mannheim, IA) by tail vessel puncture.

Tissue preparation

Mice were euthanized under isofluorane anesthesia by cervical dislocation and immediately weighed. The stomachs were removed, pinned to a Sylgard-lined dish containing 4 °C oxygenated Krebs solution, the gastric antrums were identified and acquired, and the mucosa and submucosa removed by sharp dissection (Kim et al. 2008).

SDS-PAGE and western blotting

Smooth muscles were equilibrated in oxygenated Krebs at 37 °C for 1 h. Carbachol (CCh) and KCl were added for the indicated amount of time. For western blot analysis, antrum smooth muscles were placed in ice cold acetone/10 mmol/L dithiothreitol (DTT)/10 % (w/v) trichloroacetic acid (TCA) for 2 min, snap-frozen in liquid N_2, and stored at –80 °C (Bhetwal et al. 2011; Johnson et al. 2009). The tissues were thawed on ice for 5 min, followed by three 1 min washes in ice cold acetone/10 mmol/L DTT, and a 2 min wash in ice cold lysis buffer (mmol/L; 50 Tris HCl pH 8.0, 60 beta-glycerophosphate, 100 NaF, 2 EGTA, 25 Na-pyrophosphate, 1 DTT; 1 µmol/L fasudil, 0.5 % NP-40, 0.2 % SDS, and protease inhibitor tablet (Roche, IA)) (Bhetwal et al. 2011; Johnson et al. 2009). Each tissue was homogenized in 0.15 mL lysis buffer, centrifuged at 3,000×*g* at 4 °C for 10 min, and the supernatants aliquotted and stored at –80 °C. The supernatants were analyzed by SDS-PAGE and Western blotting with anti γ-actin, LC20 (D-15), ROCK2 (H-85), MYPT1 (H-130), CPI-17 (F-4), and collagen 1 (C-18) and collagen 3 (S-17) antibodies, and phosphorylation levels were determined by Western blot analyses using anti pS19-LC20 (19849-R), pT696-MYPT1 (17556-R), pT853-MYPT1 (17432-R), and pT38-CPI-17 (17560-R) antibodies (Santa Cruz Biotechnologies, CA). The anti smooth muscle MLCK antibody (TA303608) was purchased from Origene (Rockville, MD) (The MYPT1LZ+, MYPT1LZ– antibodies were a gift from Steven A. Fisher (Univ. of Maryland). Protein bands were detected using horseradish peroxidaseconjugated secondary antibodies (Millipore-Chemicon, MA) and ECL Advance (GE HealthCare Biosciences, NJ), and visualized with a CCD camera-based detection system equipped with Visionworks software (Epi Chem II, UVP Laboratory Products, CA). The tiff images were inverted, and adjusted

to auto levels and resolution with Adobe Photoshop (CS2, V9.0.2, Adobe Systems, CA) for densitometry (Bhetwal et al. 2011).

Mechanical responses

Contractile activity was measured using standard myobath techniques, with each strip attached to a Fort 10 isometric strain gauge (WPI, FL) in parallel with the circular muscles (Bhetwal et al. 2011). A resting force of 0.6 g was applied and tissues were equilibrated for 1 h in oxygenated Krebs, followed by an additional 30 min incubation in 0.3 μmol/L tetrodotoxin prior to addition of CCh or KCl. Responses were recorded and analyzed using Acqknowledge 3.2.7 software (BIOPAC Systems, CA). At the end of the experiment the weight and length of the antrum smooth muscle tissues were measured for calculating the cross sectional area.

Calcium measurements

Following dissection, the tissues issues were pinned down onto a Sylgard-coated dish. After an equilibration period of 1 h, the preparation was loaded with Oregon Green 488 BAPTA-1 AM, 10 μg/ml (Molecular Probes, OR) in a solution of 0.02 % dimethyl sulfoxide and 0.01 % nontoxic detergent Cremophor EL for 30 min at 25 °C, followed by 15 min of incubation with wortmannin (10 μmol/L) (Sigma-Aldrich, MO) to restrict tissue movement during image acquisition. After incubation, the preparation was perfused with Krebs solution at 37 °C for 30 min to allow for dye de-esterification. Preparations were imaged using an Eclipse E600FN microscope (Nikon, Inc., NY) equipped with a number of lenses at different magnifications (X20–40, Nikon Plan Fluor). The indicator dye was excited at 488 nm, and the fluorescence emission (>515 nm) was detected using a cooled, interline transfer charge coupled device camera system (Imago, TILL Photonics, Germany). Image sequences were collected after 4×4 binning of the 344×260 line image in TILLvisION software (T.I.L.L. Photonics GmbH, Germany). Image sequences of Ca^{2+} activity in antral smooth muscle were analyzed and constructed using a custom software (Volumetry G7wv) (29). The average frequency of Ca^{2+} transients was calculated for a 60-s period after CCh or high K^+ application and under control conditions.

F-actin and G-actin analysis

The relative proportions of F-actin and G-actin in antrum smooth muscles were analyzed as previously described (Tejani et al. 2011; Zhang et al. 2010). Briefly, each tissue was homogenized in 200 μL of F-actin stabilization buffer at 37 °C (mmol/L; 50 PIPES, pH 6.9, 50 NaCl, 5 MgCl2, 5 EGTA, 1 ATP; 5 % glycerol, 0.1 % Triton X-100, 0.1 %Nonidet P-40, 0.1 % Tween-20, 0.1 % β-mercaptoethanol, 0.001 % antifoam, and protease inhibitors. Supernatants were collected by centrifugation at $150,000 \times g$ for 60 min at 37 °C. The pellets were resuspended in 200 μL of ice-cold water containing 10 μmol/L cytochalasin D and then incubated on ice for 1 h to depolymerize F-actin. The resuspended pellets were gently mixed every 15 min. Four microliter of supernatant (G-actin) and pellet (F-actin) fractions were subjected to immunoblot analysis using anti-actin antibody (clone AC-40; Sigma, MO). The relative amounts of F-actin and G-actin were determined using densitometry.

Statistical analysis

Protein concentrations were determined with the Bradford assay. Equal protein amounts were loaded for separation by SDS-PAGE. The densitometry values (pixel intensity units) of the protein bands were obtained using Vision-Works software. The densitometry values of total MYPT1, the LZ+, LZ– isoforms, pT696, pT853, CPI-17, and pT38 were obtained from the protein doublets. The densitometry values of ROCK2, MYPT1, LC20, CPI-17, and γ-actin were divided by the total microgram protein loaded into each well to obtain a relative

expression level per microgram lysate protein. This value for ROCK2, MYPT1, LC20, and CPI-17 was divided by the value for γ-actin, to obtain the expression level relative to γ-actin. Contractile actin filaments are composed of γ-actin in GI smooth muscles (Szucsik and Lessard 1995). The densitometry values of pT696, pT853, pT38, and pS19 were divided by the MYPT1, CPI-17, and LC20 densitometry values, respectively, obtained from the same sample to obtain the ratio of phosphorylated protein to total protein. Ratios were analyzed for significance by t test and are expressed as the averages ± SD. Contractile responses were measured by comparing the integral, which measures the area under the curve in a continuous fashion (amplitude units x horizontal units), per cross-sectional area (mm^2) of the smooth muscles (gram-sec). Contractile data was analyzed by one-way ANOVA and tested for significance with t test. $P < 0.05$ is considered significant.

Results

ob/ob mice are obese and hyperglycemic

As seen in Table 1, by 7 weeks of age the *ob/ob* mice weighed almost twice as much as C57BL/6 J control mice, and this difference was maintained at 12 weeks. Non-fasting blood glucose was elevated to around 350 mg/dL in 7 week old *ob/ob* mice, which declined to around 250 mg/dL by 12 weeks. A compensatory hyperplasia and hypertrophy of pancreatic beta cells is correlated with a modest remission from hyperglycemia with age in *ob/ob* mice. The resultant hyperinsulinemia is assumed to account for the remission of hyperglycemia after 12 weeks of age (Coleman 1978; Leiter 1992). The non-fasting blood glucose levels in C57BL/6 J mice remained constant at around 127 mg/dL.

Contractile responses of *ob/ob* antrum smooth muscles are impaired

The hyperglycemia and increased body weights of *ob/ob* mice at each age prompted us to compare the contractile responses of gastric antrum smooth muscles from *ob/ob* mice and age-and strain-matched control mice. At each age, the wet weight of *ob/ob* antrum smooth muscles was about 30 % greater than the controls (Tables 2, 3). However, the antrum smooth muscle weights to body weight ratios were not different. Figures 1 and 2 show the contractile characteristics of *ob/ob* and C57BL/6 J antrum smooth muscles, corrected for weight by expressing the force per unit cross sectional area. At 7 and 12 weeks of age, the peak amplitudes of the spontaneous contractions were significantly lower in antrum smooth muscles from *ob/ob* mice (Fig. 1a). At 7 weeks the amplitudes of spontaneous contractions were about 50 % lower, while at 12 weeks, they were 75 % lower (Fig. 1b). At both ages the frequencies of the spontaneous phasic contractions were about 20 % higher in *ob/ob* mice, but this difference was not significant (Fig. 1c). Analysis of the integral indicated that the force per unit cross sectional area of the spontaneous phasic contractions of *ob/ob* antrum smooth muscles was significantly reduced at each age (Fig. 1d). Similarly, at each age the mechanical responses of *ob/ob* gastric antrum smooth muscles to contractile agonists were significantly lower than the responses from the age- and strain-matched controls (Fig. 2). At 7 and 12 weeks of age, the peak amplitudes of the phasic contractions of *ob/ob* antrum smooth muscles in response to the muscarinic receptor agonist CCh (1 μmol/L, 10 μmol/L) were lower than those of the antrum smooth muscles from control mice (Fig. 2a). Similarly, the increase in tone evoked by membrane depolarization by high K^+ (70 mmol/L) was less than the increase in tone evoked in control antrum smooth muscles (Fig. 2b). The increases in force per unit cross sectional area generated by *ob/ob* antrum smooth muscles in response to CCh or high K^+ (70 mmol/L) were significantly less than the force generated by C57BL/6 J antrum smooth muscles by each agonist at each age (Fig. 2c). In control and *ob/ob* antrum smooth muscles the force per unit cross sectional area in response to CCh or high K^+ was higher at 12 weeks of age than the responses measured at 7 weeks (Fig. 2c). Despite this

increase, the contractile responses of 12 week old *ob/ob* antrum smooth muscles were still lower than the responses of 7 week old control antrum smooth muscles (Fig. 2C).

Agonist-evoked Ca^{2+} transients and MLCK expression are similar in *ob/ob* and control antrum smooth muscles

We investigated the possibility that impaired Ca^{2+} signaling and/or decreased MLCK function are responsible for the reduced mechanical responses of *ob/ob* gastric antrum smooth muscles. Intracellular Ca^{2+} oscillations were imaged and the frequencies and amplitudes of the Ca^{2+} transients evoked by CCh or high K^+ were measured. MLCK protein expression was measured by Western blot analysis. As indicated in Fig. 3, the frequencies and amplitudes of the Ca^{2+} transients evoked by CCh or high K^+ stimulation were not reduced in *ob/ob* antrum smooth muscles at both ages. In addition, there was no statistically significant difference in MLCK expression between *ob/ob* and control antrum smooth muscles at each age (Fig. 3e).

ROCK2 expression is reduced in *ob/ob* antrum smooth muscles

Since both Ca^{2+} signaling and MLCK expression are not impaired in *ob/ob* antrum smooth muscles, we examined whether the expression of Ca^{2+} sensitization and contractile proteins are altered in *ob/ob* antrum smooth muscles. Figure 4 shows representative Western blots and the expression levels of ROCK2, MYPT1, CPI-17, and LC20 relative to γ-actin calculated from the densitometry values. At each age there was no difference in LC20 (Fig. 4a), CPI-17 (Fig. 4b), or MYPT1 (Fig. 4c) expression between *ob/ob* and control antrum smooth muscles. MYPT1 and CPI-17 expression did not change between 7 and 12 weeks, while LC20 expression significantly increased in both *ob/ob* and control antrum smooth muscles between 7 and 12 weeks of age. The LZ-MYPT1:LZ + MYPT1 ratio was similar at 7 and 12 weeks in control antrum smooth muscles, but LZ-MYPT1 expression was decreased at 12 weeks in *ob/ob* antrum smooth muscles (Fig. 4c). In contrast, ROCK2 expression (Fig. 4d) was dramatically decreased in *ob/ob* antrum smooth muscles to levels approximately 50 % lower than the controls at each age.

Phosphorylation of MYPT1, but not CPI-17, is reduced in *ob/ob* antrum smooth muscles

Because of the finding that ROCK2 expression is significantly reduced in *ob/ob* antrum smooth muscles we examined whether MYPT-1 and CPI-17 phosphorylation, which are substrates of ROCK2, is reduced in *ob/ob* antrum smooth muscles (Ichikawa et al. 1996; Kitazawa et al. 2000). Basal MYPT1 phosphorylation at T696 (pT696) is reduced in *ob/ob* antrum smooth muscles at 7 and 12 weeks (Fig. 5a,b), while basal MYPT1 phosphorylation at T853 (pT853) is reduced only at 12 weeks of age (Fig. 5c,d). Basal CPI-17 phosphorylation levels at T38 (pT38) are similar in C57BL/6 J and *ob/ob* antrum smooth muscles at both ages (Fig. 5e,f). The pT696, pT853, and pT38 levels were all significantly increased from their basal levels in response to CCh (1 µmol/L, 10 µmol/L) or high K^+ (70 mmol/L) in C57BL/6 J and *ob/ob* antrum smooth muscles at both ages (Fig. 5). The increases in the pT696 levels in response to CCh or high K^+ were significantly lower in *ob/ob* antrum smooth muscles compared to the controls at 7 weeks, but were not different from controls at 12 weeks (Fig. 5a,b). The increase in pT853 was significantly lower in *ob/ob* antrum smooth muscles in response to 1 µmol/L CCh, but not 10 µmol/L CCh or high K^+, at 7 weeks of age (Fig. 5 c,d). At 12 weeks of age the increase in pT853 was significantly lower in *ob/ob* antrum smooth muscles in response to 1 µmol/L and 10 µmol/L CCh, but not high K^+ (Fig. 5c,d). The increases in pT38 levels in response to 1 µmol/L and 10 µmol/L CCh, and high K^+ were similar in control and *ob/ob* antrum smooth muscles at 7 and 12 weeks of age (Fig. 5e,f).

LC20 phosphorylation is reduced in *ob/ob* antrum smooth muscles

Because of the finding that the increases in pT696 and pT853 levels in response to CCh stimulation are attenuated in *ob/ob* antrum smooth muscles we examined whether the increase in LC20 phosphorylation evoked by CCh, which positively correlates with MYPT1 phosphorylation, is also attenuated in *ob/ob* antrum smooth muscles (Khromov et al. 2009). The basal phosphorylation levels of LC20 at S19 (pS19) are similar in *ob/ob* and control antrum smooth muscles at 7 weeks, but the basal pS19 level is reduced in *ob/ob* antrum smooth muscles at 12 weeks of age (Fig. 6a,b). The pS19 levels were significantly increased from their basal levels in response to CCh (1 µmol/L, 10 µmol/L) or high K^+ (70 mmol/L) in C57BL/6 J and *ob/ob* antrum smooth muscles at both ages (Fig. 6). The increase in pS19 was significantly lower in *ob/ob* antrum smooth muscles in response to 1 µmol/L CCh, but not 10 µmol/L CCh or high K^+, at 7 weeks of age (Fig. 6a). Similarly, at 12 weeks of age the increase in pS19 was significantly lower in *ob/ob* antrum smooth muscles in response to 1 µmol/L CCh, but not 10 µmol/L CCh or high K^+ (Fig. 6b).

The F-actin:G-actin ratios are similar in *ob/ob* and control antrum smooth muscles

Reduced actin polymerization inhibits tension development in a number of smooth muscles in response to contractile agonists (Tejani et al. 2011; Zhang et al. 2010). Since reduced contractile responses were not always associated with reduced MYPT1 and CPI-17 phosphorylation, we determined the F-actin:G-actin ratio in C57BL/6 J and *ob/ob* antrum smooth muscles using an antibody that recognizes a C-terminal epitope conserved in all actin isoforms (Fig. 7). At 7 weeks of age, there is no difference between the F-actin:G-actin ratios in control and *ob/ob* gastric antrum smooth muscles. The F-actin:G-actin ratio in C57BL/6 J antrum smooth muscles increased between 7 and 12 weeks, but this increase was not statistically significant. The F-actin:G-actin ratio did not change between 7 and 12 weeks in ob antrum smooth muscles, and was not statistically different from the 12 week ratio in C57BL/6 J controls.

Discussion

Impaired Ca^{2+} sensitization protein expression and activation is associated with reduced smooth muscle contractile responses, and has been reported in intestinal motility disorders (Depoortere et al. 2010; Godoy and Rattan 2011; Ohama et al. 2003; Sato et al. 2007). However, alterations to Ca^{2+} sensitization mechanisms in diabetic gastroparesis have not been reported. Since *ob/ob* mice develop delayed gastric emptying (Asakawa et al. 2003), we investigated the potential contribution of impaired Ca^{2+} sensitization to the reduced contractile responses of *ob/ob* antrum smooth muscles. The most striking finding was that ROCK2 expression was reduced by approximately 50 % in *ob/ob* antrum smooth muscles at both ages, suggesting that ROCK2 function is impaired. Despite the reduced ROCK2 expression, basal pT853 levels in control and *ob/ob* antrum smooth muscles at 7 weeks were similar. However, the increases in pT853 levels evoked by 1 µmol/L CCh were attenuated in *ob/ob* antrum smooth muscles at 7 weeks. Although ROCK2 expression is reduced, the remaining ROCK2 function may be able to maintain basal levels of pT853, but not able to increase pT853 levels to the control levels in response to 1 µmol/L CCh. In fact, a stronger stimulus from 10 µmol/L CCh was necessary to increase pT853 in *ob/ob* antrum smooth muscles to levels similar to controls at 7 weeks. In support of this conclusion, by 12 weeks basal pT853 levels are reduced in *ob/ob* antrum smooth muscles and 10 µmol/L CCh is not able to increase pT853 in *ob/ob* antrum smooth muscles to control levels, due to the persistent decrease in ROCK2 expression. The increases in pT853 levels evoked by high K^+ in control and *ob/ob* antrum smooth muscles were smaller than those evoked by CCh, consistent with findings indicating that ROCK2 activation by muscarinic receptors is more

robust than by membrane depolarization and activation of voltage-dependent Ca^{2+} channels (Somlyo and Somlyo 2003).

In contrast to pT853, basal MYPT1 phosphorylation at T696 was reduced in *ob/ob* antrum smooth muscles at 7 weeks. In addition, the increases in pT696 evoked by 1 μmol/L and 10 μmol/L CCh, and high K^+ in *ob/ob* antrum smooth muscles were reduced, never becoming greater than the basal pT696 levels in control antrum smooth muscles. Consistent with reduced basal and agonist-evoked pT696 levels, the force generated by the spontaneous and agonist-evoked contractions of antrum smooth muscles from the 7 week old *ob/ob* mice were reduced compared to the age-matched controls. However, at 7 weeks of age, the expression and phosphorylation of CPI-17, the other MLCP inhibitor protein, was similar to the age matched controls. Basal pT38 levels and the increases in pT38 evoked by 1 μmol/L and 10 μmol/L CCh, and high K^+ in *ob/ob* antrum smooth muscles were not different from the age-matched controls. At 12 weeks of age pT696 levels are reduced, but the increases in pT696 levels evoked by 1 μmol/L and 10 μmol/L CCh and high K^+ in control and *ob/ob* antrum smooth muscles were similar, suggesting the recovery of the pT696 phosphorylation mechanism, or the involvement of an unknown compensatory mechanism. We found that the Rho kinase inhibitor Y27632 does not reduce basal MYPT1 T696 phosphorylation in antrum smooth muscles, suggesting that ROCK2 is not involved in maintaining basal T696 phosphorylation in this tissue (Bhetwal et al. 2011). These findings are consistent with reports that ROCK2 preferentially phosphorylates T853, and that additional kinases phosphorylate T696, including MYPT1 kinase, integrin-linked kinase, myotonic dystrophy protein kinase, p21-activated protein kinase, and Raf-1 (Alvarez et al. 2010; Johnson et al. 2009; Muranyi et al. 2005; Yoneda et al. 2005). The kinase(s) that phosphorylate T696 in gastric antrum smooth muscles have not been identified.

The MYPT1 expression levels at 7 and 12 weeks in control and *ob/ob* antrum smooth muscles were similar, indicating that the reduced pT696 and pT853 levels at each age are not due to reduced MYPT1 expression. Although there was no difference in total MYPT1 expression, the MYPT1 LZ-:LZ + ratio is reduced in *ob/ob* antrum smooth muscles at 12 weeks, indicating that LZ + MYPT1 comprises a higher proportion of the total MYPT1 in *ob/ob* antrum smooth muscles at 12 weeks of age. ROCK2 phosphorylation of MYPT1 is unlikely to be affected, since the binding of ROCK2 to MYPT1 is independent of the LZ motif (Wang et al. 2009). Smooth muscles with higher LZ + MYPT1 expression are more sensitive to relaxation by cGMP, by the association of cGMP-dependent protein with MYPT1 via the LZ motif (Yuen et al. 2011). In addition, M-RIP contains functional domains that target MLCP to actin-myosin contractile filaments, but only binds to LZ + MYPT1(Surks and Mendelsohn 2003). These findings suggest that at 12 weeks more MLCP could be targeted to actin-myosin contractile filaments by the increased proportion of LZ + MYPT1, leading to greater LC20 dephosphorylation. Such mechanisms are consistent with the reduced contractile responses and LC20 phosphorylation of *ob/ob* antrum smooth muscles at 12 weeks.

Similar to MYPT1, the CPI-17 expression levels in control and *ob/ob* antrum smooth muscles at 7 and 12 weeks were not different from each other. However, in contrast to basal MYPT1 phosphorylation at T696 and T853, basal CPI-17 phosphorylation levels at T38 in control and *ob/ob* antrum smooth muscles at 7 and 12 weeks are similar. Furthermore, the increases in pT38 levels evoked by 1 μmol/L and 10 μmol/L CCh, and high K^+ were similar in control and *ob/ob* antrum smooth muscles at both ages. PKC is the major kinase that phosphorylates CPI-17 T38 in smooth muscles (Woodsome et al. 2001). However, we found that PKC inhibitors do not reduce basal pT38 levels in antrum smooth muscles, in contrast to gastric fundus and proximal colon smooth muscles (Bhetwal et al. 2011). Other kinases, including ROCK2, ZIPK, and p21-activated kinase, have been reported to phosphorylate

CPI-17 T38, but the identity of the kinase in antrum smooth muscles is unknown (Bhetwal et al. 2011). However, our finding that CPI-17 T38 phosphorylation in *ob/ob* antrum smooth muscles is unchanged suggests that the reduction in ROCK2 expression is selective and not due to a generalized impairment in kinase activity and overall Ser/Thr protein phosphorylation.

There was no difference in LC20 expression between control and *ob/ob* antrum smooth muscles at 7 and 12 weeks of age. Between 7 and 12 weeks LC20 expression increased by about 60 % in both strains.

A corresponding increase in the force of spontaneous and agonist-evoked contractions was associated with the increase in LC20 expression. However, at each age the force generated by the spontaneous and agonist-evoked contractions of *ob/ob* antrum smooth muscles was about 50 % lower than the force generated by the controls. Reduced contractile responses were not associated with reduced LC20 and MYPT1 phosphorylation in every instance. The increases in pS19 levels evoked by high K^+ in control and *ob/ob* antrum smooth muscles were similar, consistent with findings indicating that ROCK2 activation and MYPT1 phosphorylation is less critical than CPI-17 phosphorylation to the regulation of LC20 phosphorylation evoked by membrane depolarization and activation of voltage-dependent Ca^{2+} channels (Somlyo and Somlyo 2003). The decreased force of the spontaneous contractions at 7 weeks of age was not associated with reduced LC20 phosphorylation even though MYPT1 phosphorylation was reduced. Reduced contractile responses to 1 μmol/L CCh, but not 10 μmol/L CCh, were associated with reduced MYPT1 and LC20 phosphorylation at both ages, suggesting that stronger muscarinic receptor stimulation may compensate for the reduced MYPT1 phosphorylation. MLCK expression and spontaneous and agonist-evoked intracellular Ca^{2+} oscillations were not reduced in *ob/ob* antrum smooth muscles, suggesting that impaired Ca^{2+} signaling to MLCK is not responsible for the reduced LC20 phosphorylation and reduced contractile responses. Although LC20 phosphorylation in smooth muscle is coupled to increases in $[Ca^{2+}]_i$, activation of MLCK along with inhibition of MLCP may be required for strong or sustained contractile responses (Gao et al. 2013). Reduced actin polymerization has been shown to inhibit contractile force generation in smooth muscles, suggesting an additional factor that might be involved in the reduced contractile responses of antrum smooth muscles from *ob/ob* mice (Tejani et al. 2011; Zhang et al. 2010). However, we found no differences in the F-actin:G-actin ratios in antrum smooth muscles from both strains of mice at both ages. Increased fibrosis is associated with reduced smooth muscle function and has been reported in gastric muscle biopsies from patients with diabetic gastroparesis (Kashyap and Farrugia 2010). However, we found no differences in collagen 1A or 3A expression between control and *ob/ob* antrum smooth muscles (data not shown).

CPI-17 and MYPT1 expression and phosphorylation levels are key factors in evaluating their importance in regulating MLCP activity (Murthy 2006; Ohama et al. 2007). CPI-17 expression differs among smooth muscles, and the importance of MYPT1 and CPI-17 may also differ in physiological or pathophysiological situations (Ejskjaer et al. 1999; Murthy 2006; Ohama et al. 2007). Because they each bind to the active site of MLCP, their binding is mutually exclusive, so the total MLCP is inhibited by a combination of phosphorylated MYPT1 and phosphorylated CPI-17 (Eto et al. 2004; Khromov et al. 2009). Additional studies are needed to determine how MLCP is regulated by two different phosphorylated inhibitor proteins. Our findings that the reduced contractile responses of *ob/ob* antrum smooth muscles at 7 weeks are associated with reductions in only pT696 suggest that MLCP activity or antrum smooth muscle contraction may be highly sensitive to decreases in any one of the inhibitory phosphorylation sites of MYPT1 and CPI-17. Determining which inhibitor plays the dominant role in MLCP inhibition in gastric antrum smooth muscles

could aid future studies aimed at determining the most effective way of pharmacologically inhibiting MLCP activity to overcome impaired ROCK2 function for beneficial therapeutic outcomes in gastric motility disorders such as diabetic gastroparesis.

In summary, we found important differences in the expression and phosphorylation of Ca^{2+} sensitization proteins in gastric antrum smooth muscles from *ob/ob* mice. The main findings from this study are that ROCK2 expression is significantly reduced, MYPT1 and LC20 phosphorylation evoked by a muscarinic receptor agonist are reduced, and spontaneous and agonist-induced contractions are impaired. These findings represent the first indication that defects in MYPT1 phosphorylation may contribute to the impaired gastric antrum function associated with diabetic gastroparesis.

The pathophysiology of diabetic gastroparesis is quite heterogeneous, with variable dropout of enteric neurons and ICCs, smooth muscle fibrosis, disruption of neurotransmitter synthesis, and increased inflammatory cell infiltration in the myenteric plexus (Ordog et al. 2009). A number of defects in several systems likely contribute to the impaired contractile responses of *ob/ob* antrum smooth muscles, including, as shown here, impaired Ca^{2+} sensitization responses. The mechanism underlying the reduced ROCK2 expression in gastric antrum smooth muscles from *ob/ob* mice is unknown. The hyperglycemia and hyperinsulinemia characteristic of the type 2 diabetes-like syndrome of *ob/ob* mice alters cellular signaling in a variety of systems, including gastric smooth muscles (Asakawa et al. 2003; Iizuka and Horikawa 2008). Circulating levels of cytokines and inflammatory mediators including TGF-β1 and TNF-α are elevated in *ob/ob* mice, and affect gene transcription throughout the digestive tract (Ilan et al. 2010; Samad et al. 1997). Interestingly, up-regulation of microRNAs 138, 139, and 124 decreases ROCK2 expression in carcinoma cell lines and leads to suppression of metastasis (Jiang et al. 2010; Wong et al. 2011; Zheng et al. 2012). Additional studies are required to elucidate the key factors involved in the down-regulation of ROCK2 protein expression, and determine the importance of impaired Ca^{2+} sensitization signaling to the cellular pathogenesis of diabetic gastroparesis.

Acknowledgments

References

Alvarez SM, Miner AS, Browne BM, Ratz PH. Failure of Bay K 8644 to induce RhoA kinase-dependent calcium sensitization in rabbit blood vessels. Brit J Pharmacol. 2010; 160:1326–1337. [PubMed: 20590624]

Asakawa A, Inui A, Ueno N, Makino S, Uemoto M, Fujino MA, Kasuga M. Ob/ob mice as a model of delayed gastric emptying. J Diabetes Compl. 2003; 17:27–28.

Bhetwal BP, An CL, Fisher SA, Perrino BA. Regulation of basal LC20 phosphorylation by MYPT1 and CPI-17 in murine gastric antrum, gastric fundus, and proximal colon smooth muscles. Neurogastroenterol & Motil. 2011; 23:e425–e436.

Cobine CA, Fong M, Hamilton R, Keef KD. Species dependent differences in the actions of sympathetic nerves and noradrenaline in the internal anal sphincter. Neurogastroenterol & Motil. 2007; 19:937–945.

Coleman DL. Obese and diabetes: two mutant genes causing diabetes-obesity syndromes in mice. Diabetologia. 1978; 14:141–148. [PubMed: 350680]

Depoortere I, Thijs T, Janssen S, De Smet B, Tack J. Colitis affects the smooth muscle and neural response to motilin in the rabbit antrum. Brit J Pharmacol. 2010; 159:384–393. [PubMed: 20002099]

Ejskjaer NT, Bradley JL, Buxton-Thomas MS, Edmonds ME, Howard ER, Purewal T, Thomas PK, Watkins PJ. Novel surgical treatment and gastric pathology in diabetic gastroparesis. Diabet Med. 1999; 16:488–495. [PubMed: 10391397]

Eto M, Kitazawa T, Brautigan DL. Phosphoprotein inhibitor CPI-17 specificity depends on allosteric regulation of protein phosphatase-1 by regulatory subunits. Proc Nat Acad Sci. 2004; 101:8888–8893. [PubMed: 15184667]

Fu K, Mende Y, Bhetwal BP, Baker S, Perrino BA, Wirth B, Fisher SA. Tra2b protein Is required for tissue-specific splicing of a smooth muscle myosin phosphatase targeting subunit alternative exon. J Biol Chem. 2012; 287:16575–16585. [PubMed: 22437831]

Gao N, Huang J, He W, Zhu M, Kamm KE, Stull JT. Signaling through myosin light chain kinase in smooth muscles. J Biol Chem. 2013 (Epub ahead of print).

Godoy MAF, Rattan S. Role of rho kinase in the functional and dysfunctional tonic smooth muscles. Trends Pharmacol Sci. 2011; 32:384–393. [PubMed: 21497405]

Grover M, Farrugia G, Lurken MS, Bernard CE, Faussone-Pellegrini MS, Smyrk TC, Parkman HP, Abell TL, Snape WJ, Hasler WL, Unalp-Arida A, Nguyen L, Koch KL, Calles J, Lee L, Tonascia J, Hamilton FA, Pasricha PJ. Cellular changes in diabetic and idiopathic gastroparesis. Gastroenterol. 2011; 140:1575–1585.

Hasler WL. Gastroparesis: pathogenesis, diagnosis and management. Nat Rev Gastroenterol Hepatol. 2011; 8:438–453. [PubMed: 21769117]

Hirano K. Current topics in the regulatory mechanism underlying the Ca^{2+} sensitization of the contractile apparatus in vascular smooth muscle. J Pharmacol Sci. 2007; 104:109–115. [PubMed: 17538233]

Horvath VJ, Vittal H, Lorincz A, Chen H, Almeida-Porada G, Redelman D, Ordog T. Reduced stem cell factor links smooth muscle myopathy and loss of interstitial cells of Cajal in murine diabetic gastroparesis. Gastroenterol. 2006; 130:759–770.

Ichikawa K, Ito M, Hartshorne DJ. Phosphorylation of the large subunit of myosin phosphatase and inhibition of phosphatase activity. J Biol Chem. 1996; 271:4733–4740. [PubMed: 8617739]

Iizuka K, Horikawa Y. ChREBP: a glucose-activated transcription factor involved in the development of metabolic syndrome. Endocr J. 2008; 55:617–624. [PubMed: 18490833]

Ilan Y, Maron R, Tukpah AM, Maioli TU, Murugaiyan G, Yang K, Wu HY, Weiner HL. Induction of regulatory T cells decreases adipose inflammation and alleviates insulin resistance in *ob/ob* mice. Proc Nat Acad Sci. 2010; 107:9765–9770. [PubMed: 20445103]

Ingalls AM, Dickie MM, Snell GD. Obese, a new mutation in the house mouse. J Hered. 1950; 41:317–318. [PubMed: 14824537]

Intagliata N, Koch K. Gastroparesis in type 2 diabetes mellitus: prevalence, etiology, diagnosis, and treatment. Curr Gastroenterol Rep. 2007; 9:270–279. [PubMed: 17883973]

Jiang L, Liu X, Kolokythas A, Yu J, Wang A, Heidbreder CE, Shi F, Zhou X. Downregulation of the Rho GTPase signaling pathway is involved in the microRNA-138-mediated inhibition of cell migration and invasion in tongue squamous cell carcinoma. Int J Cancer. 2010; 127:505–512. [PubMed: 20232393]

Johnson RP, El-Yazbi AF, Takeya K, Walsh EJ, Walsh MP, Cole WC. Ca^{2+} sensitization via phosphorylation of myosin phosphatase targeting subunit at threonine-855 by Rho kinase contributes to the arterial myogenic response. J Physiol. 2009; 587:2537–2553. [PubMed: 19359365]

Kashyap P, Farrugia G. Diabetic gastroparesis: what we have learned and had to unlearn in the past 5 years. Gut. 2010; 59:1716–1726. [PubMed: 20871131]

Khromov A, Choudhury N, Stevenson AS, Somlyo AV, Eto M. Phosphorylation-dependent autoinhibition of myosin light chain phosphatase accounts for Ca2 + sensitization force of smooth muscle contraction. J Biol Chem. 2009; 284:21569–21579. [PubMed: 19531490]

Kim M, Hennig GW, Smith TK, Perrino BA. Phospholamban knockout increases CaM kinase II activity and intracellular Ca2 + wave activity and alters contractile responses of murine gastric antrum. Am J Physiol Cell Physiol. 2008; 294:C432–C441. [PubMed: 18045856]

Kitazawa T, Eto M, Woodsome TP, Brautigan DL. Agonists Trigger G Protein-mediated Activation of the CPI-17 Inhibitor Phosphoprotein of Myosin Light Chain Phosphatase to Enhance Vascular Smooth Muscle Contractility. J Biol Chem. 2000; 275:9897–9900. [PubMed: 10744661]

Kovac JR, Preiksaitis HG, Sims SM. Functional and molecular analysis of L-type calcium channels in human esophagus and lower esophageal sphincter smooth muscle. Am J Physiol Gastrointest Liver Physiol. 2005; 289:G998–G1006. [PubMed: 16020652]

Leiter EH. Variation in the severity and duration of hyperglycemia in the C57BL/6 J-*ob/ob* (obese) mouse. JAX Notes. 1992; 451

Muranyi A, Derkach D, Erdodi F, Kiss A, Ito M, Hartshorne DJ. Phosphorylation of Thr695 and Thr850 on the myosin phosphatase target subunit: inhibitory effects and occurrence in A7r5 cells. FEBS Lett. 2005; 579:6611–6615. [PubMed: 16297917]

Murthy KS. Signaling for contraction and relaxation in smooth muscle of the gut. Annu Rev Physiol. 2006; 68:345–374. [PubMed: 16460276]

Murthy KS, Zhou H, Grider JR, Brautigan DL, Eto M, Makhlouf GM. Differential signalling by muscarinic receptors in smooth muscle: m2-mediated inactivation of myosin light chain kinase via Gi3, Cdc42/Rac1 and p21-activated kinase 1 pathway, and m3-mediated MLC20 (20 kDa regulatory light chain of myosin II) phosphorylation via Rho-associated kinase/myosin phosphatase targeting subunit 1 and protein kinase C/CPI-17 pathway. Biochem J. 2003; 374:145–155. [PubMed: 12733988]

Ohama T, Hori M, Sato K, Ozaki H, Karaki H. Chronic treatment with interleukin-1b attenuates contractions by decreasing the activities of CPI-17 and MYPT-1 in intestinal smooth muscle. J Biol Chem. 2003; 278:48794–48804. [PubMed: 14512413]

Ohama T, Hori M, Momotani E, Iwakura Y, Guo F, Kishi H, Ozaki H. Intestinal inflammation downregulates smooth muscle CPI-17 through induction of TNF-alpha and causes motility disorders. Am J Physiol Gastrointest Liver Physiol. 2007; 292:G1429–G1438. [PubMed: 17307724]

Ordog T, Takayama I, Cheung WK, Ward SM, Sanders KM. Remodeling of networks of interstitial cells of Cajal in a murine model of diabetic gastroparesis. Diabetes. 2000; 49:1731–1739. [PubMed: 11016458]

Ordog T, Hayashi Y, Gibbons SJ. Cellular pathogenesis of diabetic gastroenteropathy. Minerva Gastroenterolica Diabetica. 2009; 55:315–342.

Parkman HP, Hasler WL, Fisher RS. American Gastroenterological Association technical review on the diagnosis and treatment of gastroparesis. Gastroenterol. 2004; 127:1592–1622.

Patel CA, Rattan S. Spontaneously tonic smooth muscle has characteristically higher levels of RhoA/ROK compared with the phasic smooth muscle. Am J Physiol Gastrointest Liver Physiol. 2006; 291:G830–G837. [PubMed: 16763289]

Rattan S, Phillips BR, Maxwell PJ. RhoA/Rho-kinase: pathophysiologic and therapeutic implications in gastrointestinal smooth muscle tone and relaxation. Gastroenterol. 2010; 138:13–18.

Rich A, Kenyon JL, Hume JR, Overturf K, Horowitz B, Sanders KM. Dihydropyridine-sensitive calcium channels expressed in canine colonic smooth muscle cells. Am J Physiol. 1993; 264:C745–C754. [PubMed: 7681626]

Riddick N, Ki O, Surks HK. Targeting by myosin phosphatase-RhoA interacting protein mediates RhoA/ROCK regulation of myosin phosphatase. J Cell Biochem. 2008; 103:1158–1170. [PubMed: 17661354]

Samad F, Yamamoto K, Pandey M, Loskutoff DJ. Elevated expression of transforming growth factor-beta in adipose tissue from obese mice. Mol Med. 1997; 3:37–48. [PubMed: 9132278]

Sanders KM. Regulation of smooth muscle excitation and contraction. Neurogastroenterol & Motil. 2008; 20:39–53.

Sato K, Ohkura S, Kitahara Y, Ohama T, Hori M, Sato M, Kobayashi S, Sasaki Y, Hayashi T, Nasu T, Ozaki H. Involvement of CPI-17 downregulation in the dysmotility of the colon from dextran

sodium sulphate-induced experimental colitis in a mouse model. Neurogastroenterol & Motil. 2007; 19:504–514.

Somlyo AP, Somlyo AV. Ca2 + sensitivity of smooth muscle and nonmuscle myosin II: modulated by G proteins, kinases, and myosin phosphatase. Physiol Rev. 2003; 83:1325–1358. [PubMed: 14506307]

Soykan I, Sivri B, Sarosiek I, Kiernan B, Mccallum RW. Demography, clinical character-istics, psychological and abuse profiles, treatment, and long-term follow-up of patients with gastroparesis. Dig Dis Sci. 1998; 43:2398–2404. [PubMed: 9824125]

Surks HK, Mendelsohn ME. Dimerization of cGMP-dependent protein kinase 1a and the myosin-binding subunit of myosin phosphatase: role of leucine zipper domains. Cell Sig. 2003; 15:937–944.

Szucsik JC, Lessard JL. Cloning and sequence analysis of the mouse smooth muscle g-enteric actin gene. Genomics. 1995; 28:154–162. [PubMed: 8530021]

Tejani AD, Walsh MP, Rembold CM. Tissue length modulates "stimulated actin polymerization," force augmentation, and the rate of swine carotid arterial contraction. Am J Physiol - Cell Physiol. 2011; 301:C1470–C1478. [PubMed: 21865586]

Wang YR, Fisher RS, Parkman HP. Gastroparesis-related hospitalizations in the United States: trends, characteristics, and cutcomes, 1995–2004. Am J Gastroenterol. 2008; 103:313–322. [PubMed: 18047541]

Wang Y, Zheng XR, Riddick N, Bryden M, Baur W, Zhang X, Surks HK. ROCK isoform regulation of myosin phosphatase and contractility in vascular smooth muscle cells. Circ Res. 2009; 104:531–540. [PubMed: 19131646]

Wegener JW, Schulla V, Koller A, Klugbauer N, Feil R, Hofmann F. Control of intestinal motility by the Ca(v)1.2 L-type calcium channel in mice. FASEB J. 2006; 20:1260–1262. [PubMed: 16636102]

Wong CC-L, Wong C, Tung EK, Au SL, Lee JM, Poon RT, Man K, Ng IO. The MicroRNA miR-139 suppresses metastasis and progression of hepatocellular carcinoma by down-regulating Rho-kinase 2. Gastroenterol. 2011; 140:322–331.

Woodsome TP, Eto M, Everett A, Brautigan DL, Kitazawa T. Expression of CPI-17 and myosin phosphatase correlates with Ca^{2+} sensitivity of protein kinase C-induced contraction in rabbit smooth muscle. J Physiol. 2001; 535:553–564. [PubMed: 11533144]

Xue L, Suzuki H. Electrical responses of gastric smooth muscles in streptozotocin-induced diabetic rats. Am J Physiol Gastrointest Liver Physiol. 1997; 272:G77–G83.

Yamamoto T, Watabe K, Nakahara M, Ogiyama H, Kiyohara T, Tsutsui S, Tamura S, Shinomura Y, Hayashi N. Disturbed gastrointestinal motility and decreased interstitial cells of Cajal in diabetic db/db mice. J Gastroenterol Hepatol. 2008; 23:660–667. [PubMed: 18341539]

Yoneda A, Multhaupt HAB, Couchman JR. The Rho kinases I and II regulate different aspects of myosin II activity. J Cell Biol. 2005; 170:443–453. [PubMed: 16043513]

Yuen S, Ogut O, Brozovich FV. MYPT1 Protein isoforms are differentially phosphorylated by protein kinase G. J Biol Chem. 2011; 286:37274–37279. [PubMed: 21890627]

Zhang W, Du L, Gunst SJ. The effects of the small GTPase RhoA on the muscarinic contraction of airway smooth muscle result from its role in regulating actin polymerization. Am J Physiol Cell Physiol. 2010; 299:C298–C306. [PubMed: 20445174]

Zheng F, Liao YJ, Cai MY, Liu YH, Liu TH, Chen SP, Bian XW, Guan XY, Lin MC, Zeng YX, Kung HF, Xie D. The putative tumour suppressor microRNA-124 modulates hepato-cellular carcinoma cell aggressiveness by repressing ROCK2 and EZH2. Gut. 2012; 61:278–289. [PubMed: 21672940]
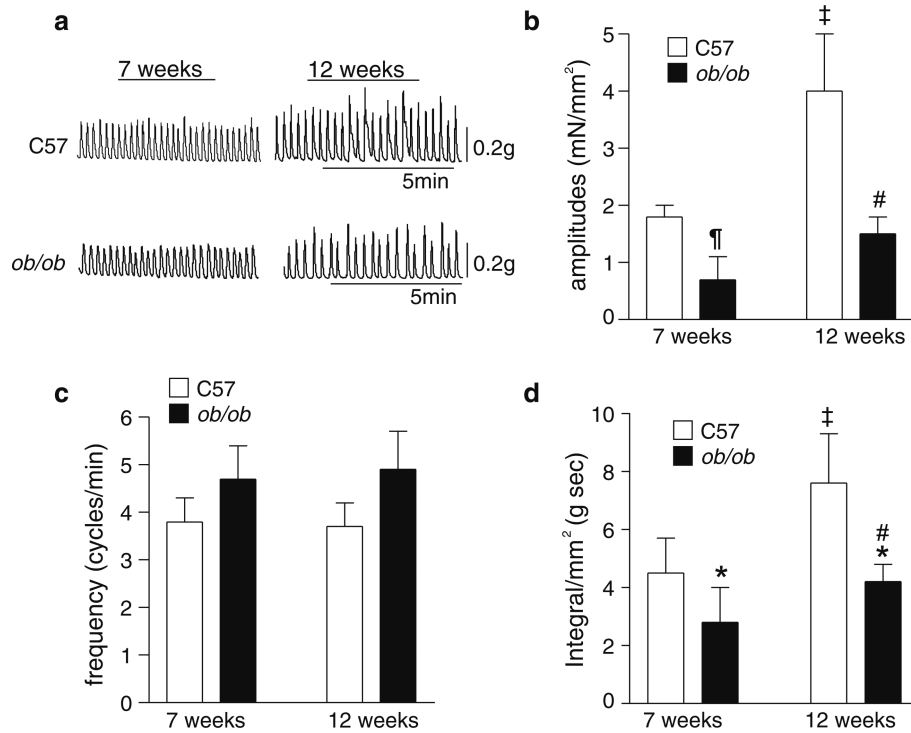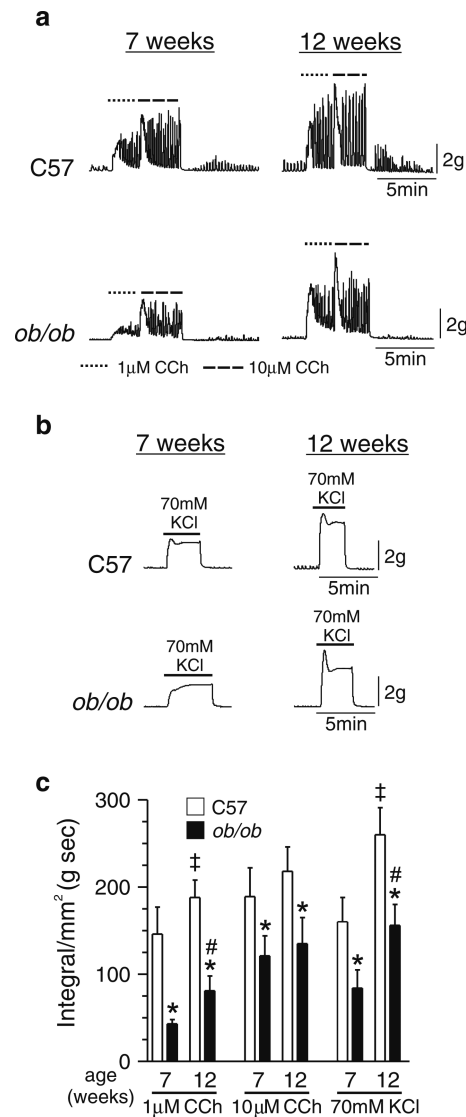
Fig. 1.
Spontaneous phasic contractions of gastric antrum smooth muscles from *ob/ob* mice generate less force per unit cross sectional area than wild-type gastric antrum smooth muscles. **a** Representative recordings of spontaneous phasic contractions in the presence of tetrodotoxin. Average values of the amplitudes (**b**), frequencies (**c**), and integrals (**d**) of spontaneous phasic contractions. $n = 6$, each strain, each age. $*P < 0.01$, compared to age-matched control. $\P P < 0.05$, compared to age-matched control. $\ddagger P < 0.01$, compared to 7 weeks C57BL/6J. $\# P < 0.01$, compared to 7 weeks *ob/ob*

Fig. 2.
Gastric antrum smooth muscles from *ob/ob* mice generate less force per cross sectional unit area than wild-type gastric antrum smooth muscles in response to receptor stimulation by CCh, or depolarization by high K^+. **a** Representative recordings of contractions evoked by 1 μmol/L CCh (*dotted line*) and the cumulative addition of 10 μmol/L CCh (*dashed line*). **b** Representative recordings of contractions evoked by high K^+ (70 mmol/L). **c** Average values of the integrals of CCh-and high K^+-evoked contractions. $n = 6$, each strain, each age. *Compared to age-matched control, $P < 0.01$. ‡Compared to 7 weeks C57BL/6 J, $P < 0.01$. #Compared to 7 weeks *ob/ob*, $P < 0.01$
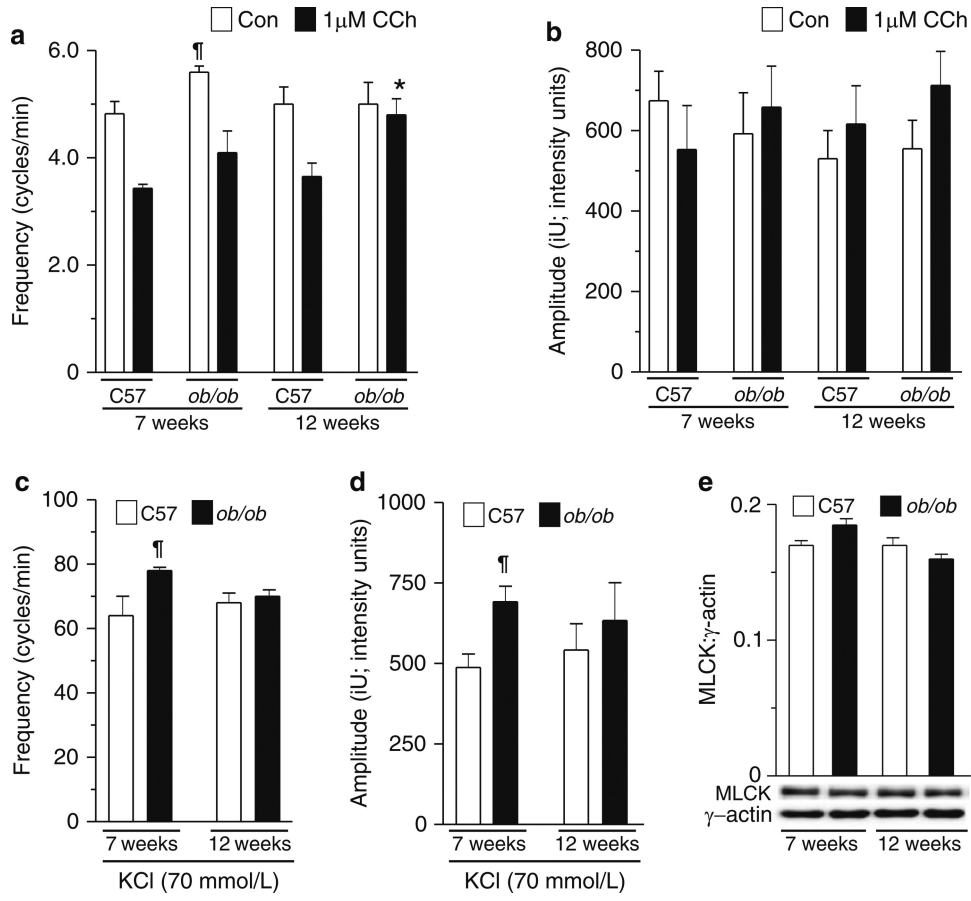
Fig. 3.
Spontaneous and agonist-evoked Ca^{2+} transients are not reduced in 7 and 12 week old *ob/ob* gastric antrum smooth muscles. Ca^{2+} transients were detected with Oregon Green 488 BAPTA-1 AM (10 µg/ml) by excitation at 488 nm and capturing the fluorescence emission at >515 nm. Average values of the **a** frequencies and **b** amplitudes of the spontaneous and CCh-evoked (1 µmol/L) Ca^{2+} transients. Average values of the **c** frequencies and **d** amplitudes of the Ca^{2+} transients evoked by 70 mmol/L KCl. **e** Upper panel, average values of the ratios of MLCK expression relative to γ-actin. $P > 0.05$. Lower panels, representative western blots, 10 µg protein/lane. $n = 4$, each strain, each age. ¶$P < 0.05$, compared to age-matched control
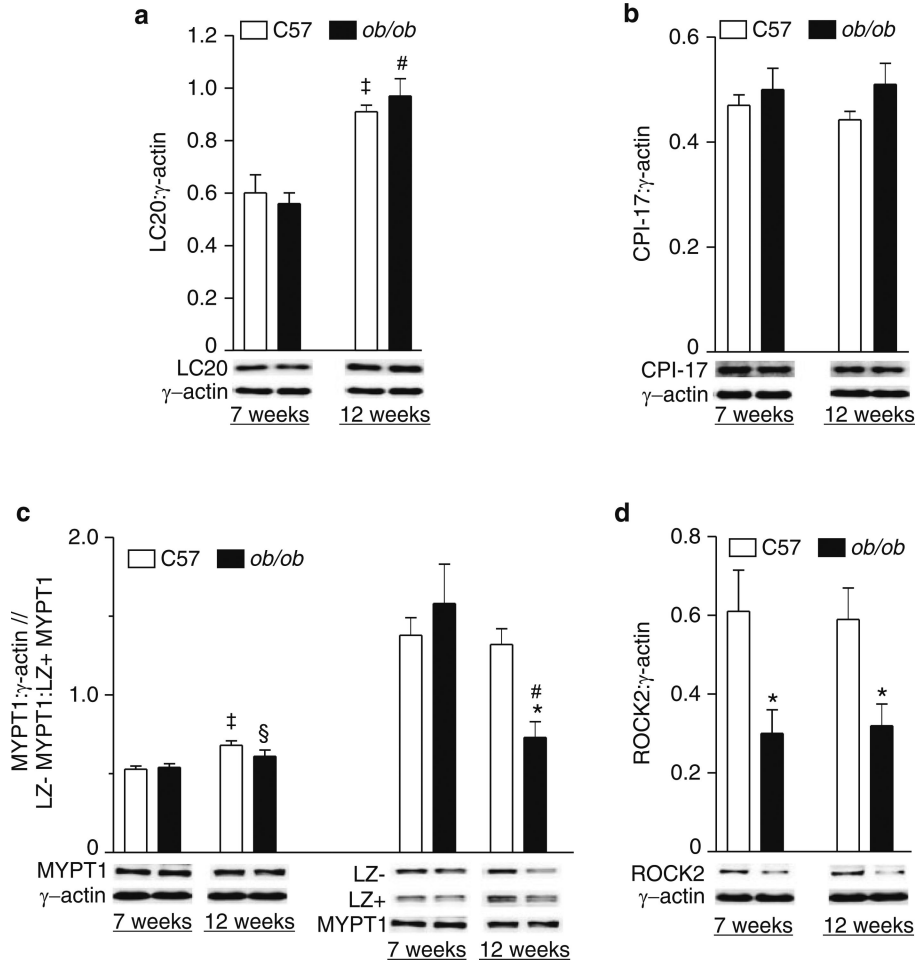
Fig. 4.
Expression levels of LC20, CPI-17, MYPT1, and ROCK2 in gastric antrum smooth muscles from 7 to 12 week old C57BL/6 J mice and *ob/ob* mice. The densitometry values (pixel intensity units) of the protein bands were divided by the total microgram protein loaded into each well to obtain a relative expression level per microgram lysate protein. This value for ROCK2, MYPT1, LC20, and CPI-17 was divided by the value for γ-actin, to obtain the expression level relative to γ-actin. *Upper panels*, average values of the ratios of **a** LC20, **b** CPI-17, **c** MYPT1, and **d** ROCK2 expression relative to γ-actin. **c** Average values of the ratios of expression of LZ+ MYPT and LZ– MYPT1 relative to MYPT1, *upper panel*. *Lower panels*, representative western blots, 10 μg protein/lane for each protein. $n = 6$, each strain, each age. *$P < 0.01$, compared to age-matched control. ‡$P < 0.01$ compared to 7 weeks C57BL/6 J, #$P < 0.01$ compared to 7 weeks *ob/ob*. §$P < 0.05$ compared to 7 weeks *ob/ob*
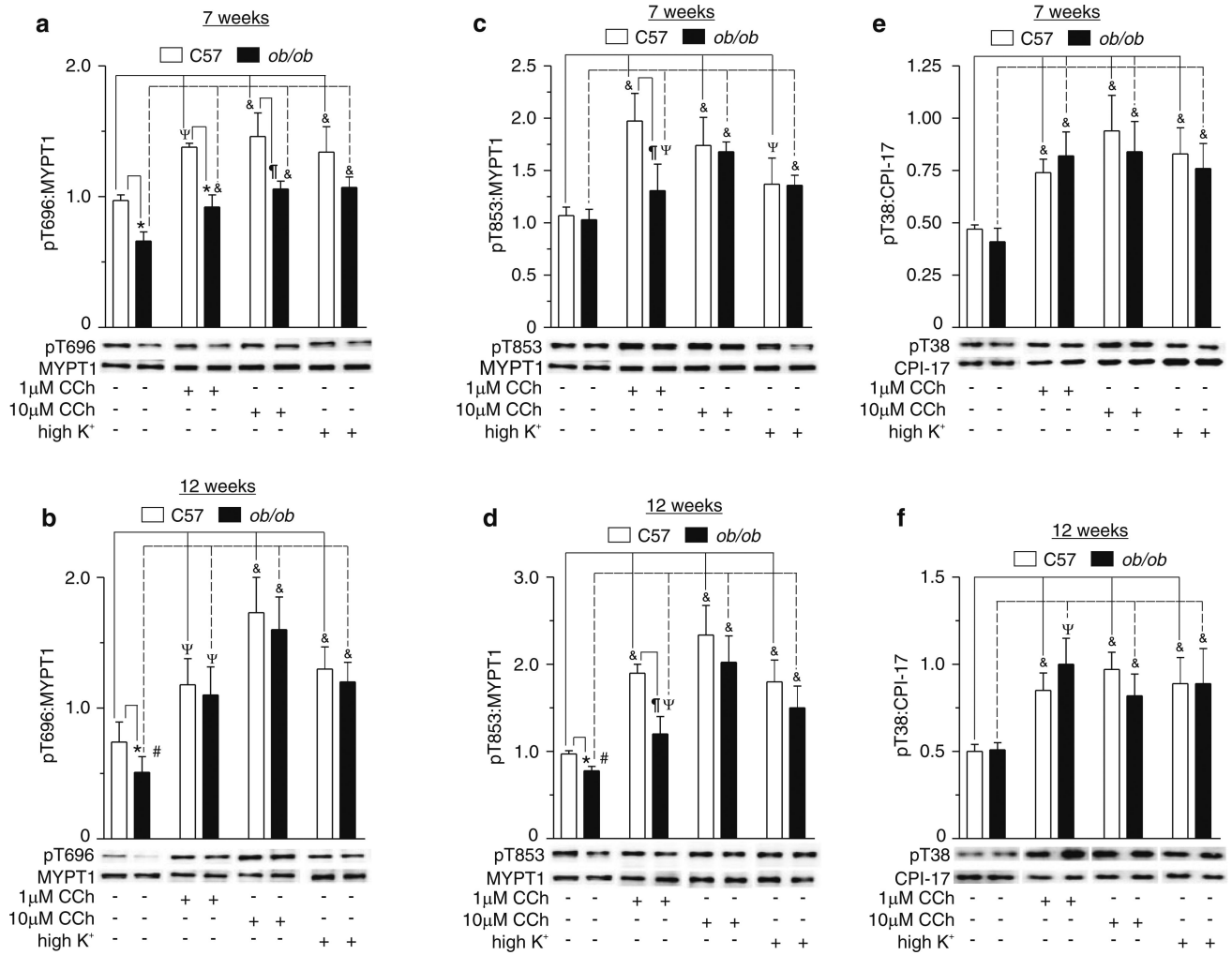
Fig. 5.
Basal and agonist-evoked MYPT1 and CPI-17 phosphorylation in gastric antrum smooth
muscles from 7 to 12 week old C57BL/6 J and *ob/ob* mice. The densitometry values (pixel
intensity units) of the phospho-protein bands were divided by the corresponding
densitometry values for MYPT1 and CPI-17 to obtain the phospho-protein to total protein
ratios. *Upper panels*, average values of the pT696:MYPT1 (**a** 7 weeks; **b** 12 weeks),
pT853:MYPT1 (**c** 7 weeks; **d** 12 weeks), and pT38:CPI-17 (**e** 7 weeks; **f** 12 weeks) ratios.
Lower panels, representative western blots, 10 μg protein/lane for each protein. $n = 6$, each
strain, each age. *$P < 0.01$, compared to C57BL/6 J. ¶$P < 0.05$, compared to C57BL/6 J. #$P
< 0.01$ compared to 7 weeks *ob/ob*. &$P < 0.001$, compared to the basal ratio. Ψ$P < 0.05$,
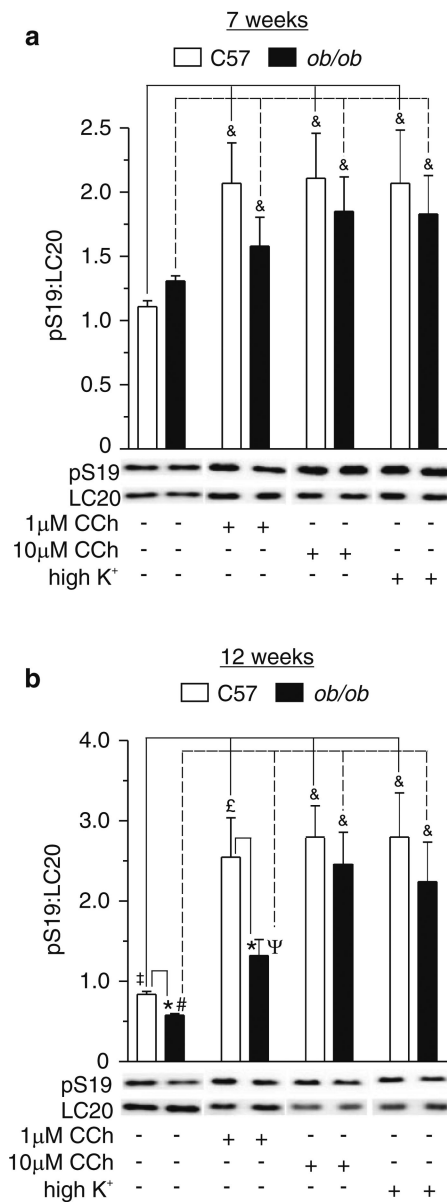compared to the basal ratio

Fig. 6.
Basal and agonist-evoked LC20 phosphorylation in gastric antrum smooth muscles from 7 to 12 week old C57BL/6 J mice and *ob/ob* mice. The densitometry values (pixel intensity units) of the phospho-LC20 (pS19) band was divided by the corresponding densitometry values for LC20 to obtain the phospho-LC20 to total protein ratios. Upper panels, average values of the pS19:LC20 ratios (**a** 7 weeks; **b** 12 weeks). *Lower panels*, representative western blots, 10 μg protein/lane for each protein. $n = 6$, each strain, each age. *$P < 0.01$, compared to C57BL/6 J. ‡$P < 0.01$, compared to 7 weeks C57BL/6 J. #$P < 0.01$, compared to 7 weeks *ob/ob*. &$P < 0.001$, compared to the basal ratio. £$P < 0.01$, compared to the basal ratio. Ψ$P < 0.05$, compared to the basal ratio
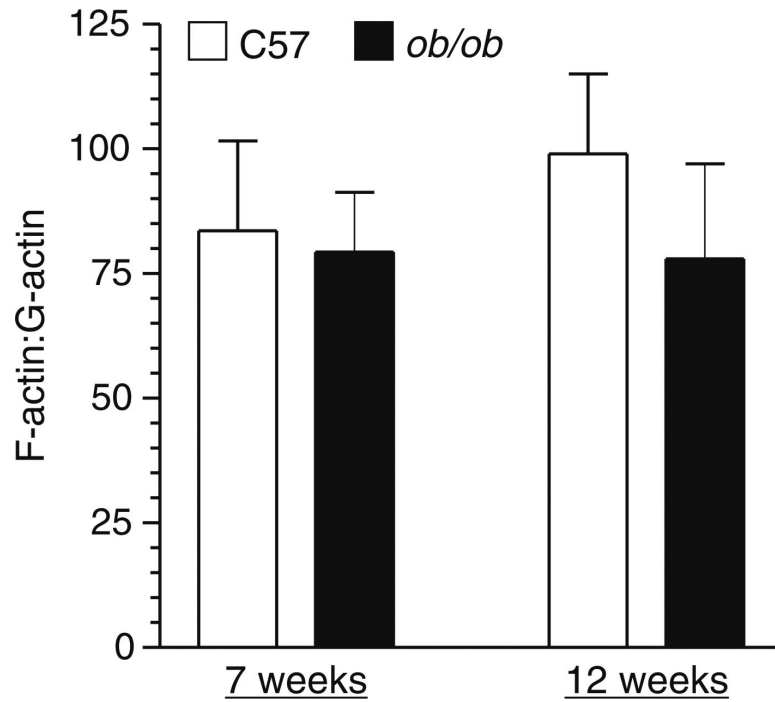
Fig. 7.
The F-actin:G-actin ratios in gastric antrum smooth muscles from each strain are not significantly different from each other at each age. High speed centrifugation of lysates at room temperature in cytoskeleton stabilization buffer was used to obtain The G-actin (supernatant) and F-actin (pellet) fractions for immunoblot analysis with the anti-actin antibody (clone AC-40; Sigma, MO). The relative amounts of F-actin and G-actin were determined using densitometry. $n = 6$, each strain, each age. $P > 0.05$

Table 1

Body weights and blood glucose levels of C57BL/6 and *ob/ob* mice

	7 weeks	12 weeks
Weight (g)		
C57	23 ± 3	28 ± 2
ob/ob	43 ± 5 *	53 ± 3 *,#
Blood glucose (mg/dL)		
C57	127 ± 19	127 ± 18
ob/ob	348 ± 51 *	251 ± 86 *,#

n = 15, each strain, each age

*
P < 0.01, compared to age-matched control.

#
P < 0.01, compared to 7 weeks *ob/ob*

Table 2

Gastric antrum smooth muscle wet weight and antrum smooth muscle weight:body weight ratios of C57BL/6 and *ob/ob* mice

		7 weeks	**12 weeks**
Antrum (mg)	C57	8.9 ± 0.6	10.2 ± 0.9
	ob/ob	$12.3 \pm 0.9^{*}$	$15.3 \pm 0.9^{*,\#}$
Antrum (mg)	C57	0.39 ± 0.16	0.28 ± 0.11
Body (g)	*ob/ob*	$0.36 \pm 0.14^{*}$	$0.29 \pm 0.13^{*,\#}$

$n = 6$, each strain, each age

*$P < 0.01$, compared to age-matched control.

#$P < 0.01$, compared to 7 weeks *ob/ob*

Table 3

γ-Actin expression in gastric antrum smooth muscles from C57BL/6 and *ob/ob* mice

		7 weeks	12 weeks
γ-Actin/10^{-6}g	C57	$3.2 \times 10^6 \pm 6.5 \times 10^5$ iu	$2.8 \times 10^6 \pm 4.4 \times 10^5$ iu
	ob/ob	$3.4 \times 10^6 \pm 6.4 \times 10^5$ iu	$3.1 \times 10^6 \pm 5.9 \times 10^5$ iu

iu intensity units. *n* = 15, each strain, each age